IAENG International Journal of Applied Mathematics

Fast Risk Estimation through Fourier Transform Based Multilevel Monte Carlo Simulation

Jia-Chen Wan

***Abstract*—In this paper, we consider a problem of estimating a large loss probability of financial derivatives portfolio, which are commonly modeled as nested expectations. However, the cost of nested simulation may be too expensive and thus multilevel Monte Carlo (MLMC) method is recently used to reduce the nested simulation complexity. When using antithetic MLMC to solve the indicator function, we get the complexity of $O(\epsilon^{-5/2})$. To decrease the computational burden, we use a Fourier transform method to modify the form of indicator function. The new estimator is sufficiently smooth and enables the antithetic MLMC method to achieve a better complexity. In addtion, we combine quasi-Monte Carlo (QMC) with MLMC to reduce the variance of inner estimator. Numerical results show that using the Fourier transform method in both MLMC and MLQMC can attain the optimal complexity $O(\epsilon^{-2})$.**

***Index Terms*—nested simulation, multilevel Monte Carlo, quasi-Monte Carlo, Fourier transform.**

I. Introduction

ASSUMING we have a portfolio which consists of some financial derivatives. Let $V(t)$ denote the present value of this portfolio at time t, where $\triangle t$ denotes the duration between successive points in time and $V(t+\triangle t)$ represents the future value of the portfolio at time $t+\triangle t$. It is important to note that $\triangle t$ corresponds to the period of time over which the portfolio will be held or managed. In order to investigate the investment issue, Deng, Lin and Zhuang [1] employed possibilistic theory and fuzzy investment to address the uncertainty of the portfolio. Conversely, we utilized a simulation method to determine the likelihood of significant losses. In this paper, the portfolio value loss is defined by $\triangle V \equiv V(t) - V(t+\triangle t)$. In this paper, we consider the problem of estimating

$$F(c) = \mathbb{P}(\triangle V \leq c) = \mathbb{E}[\mathbb{I}\{\triangle V \leq c\}] = \mathbb{E}[\mathbb{I}\{\mathbb{E}[X|Y] \leq c\}], \tag{1}$$

where the inner expectation

$$\triangle V = \mathbb{E}[X|Y], \tag{2}$$

is the change of portfolio value and c is a predetermined loss threshold, $F(c)$ is the cumulative function (c.d.f) of $\triangle V$. For a given level of confidence $\alpha \in (0,1)$, the value-at-risk (VaR) is defined as follows:

$$\xi_\alpha = F^{-1}(\alpha) = \inf\{\alpha : F(x) \geq \alpha\}. \tag{3}$$

To estimate (1), nested simulation, also known as two-stage stochastic-on-stochastic simulation, involving an outer and inner stage, can be employed straightforwardly. In the outer stage, we simulate risk factors that span a specific risk horizon known as Y. This is referred to the scenarios. In the inner stage, for each scenario Y, we generate numerous corresponding X values, which are then used to estimate the conditional expectation $\mathbb{E}[X|Y]$, see Gordy and Juneja [2] and Broadie et al. [3] for details. Similarly, regarding the financial risk management problem, Li and Wen [4] based on federated learning to obtain a credit risk measure.

The standard nested Monte Carlo simulation imposes a heavy computational burden. To address this issue, Gordy and Juneja [2] analyzed the optimal allocation of computational resources between the inner and outer stages. By minimizing the root mean square error (RMSE) ϵ of the resulting estimator, they obtained the most appropriate computational cost allocation: the outer stage sample size is $N = O(\epsilon^{-2})$ and the inner stage sample size is $M = O(\epsilon^{-1})$, yielding in a total cost of $NM = O(\epsilon^{-3})$. More efficiently, Broadie et al. [3] developed a clever procedure to adaptively allocate methods in the inner stage based on marginal changes of the risk estimator in each scenario. Min, Han and Xiang [5] has proposed a robust omega portfolio optimization for solving the two-stage portfolio problem. Many work have focused on reducing the computational burden of the inner stage by using approximation techniques. For example, Broadie et al. [6] introduced the least square Monte Carlo method to estimate portfolio risk, and Hong et al. [7] developed a kernel smoothing method.

However, the earlier methods mentioned have certain limitations. In order to enhance computational efficiency, Giles [8] used a multigrid idea that differs from Gordy and Juneja [2], Broadie et al. [3] and Hong et al. [7]. Giles and Szpruch proposed a multilevel Monte Carlo method (MLMC) to solve nested expectations denoted by stochastic differential equations [9]. This work successfully reduced the total cost of nested simulation to $O(\epsilon^{-2}\log\epsilon^2)$ under special circumstances. Recently, Giles and Haji-Ali [10] employed the adaptive allocation procedure of Broadie et al. [3] to address the risk estimation problem and demonstrated that the complexity of MLMC can be reduced to $O(\epsilon^{-2}\log\epsilon^2)$ under specific conditions. Giles and Haji-Ali [10] showed that the complexity of antithetic MLMC is $O(\epsilon^{-5/2})$ for the risk estimation problem (1). Due to the discontinuity of the indicator function, antithetic MLMC cannot achieve the optimal complexity of $O(\epsilon^{-2})$ for the problem (1). For some nested MLMC methods, we refer to Giles [11]; Giles and Goda [12]; Goda et al. [13] [14] and references therein.

As mentioned earlier, the calculation complexity of

Manuscript received September 8, 2023; revised January 23, 2024.
Jia-Chen Wan is a postgraduate student of the School of Mathematics, South China University of Technology, Guangzhou 510640, China (e-mail: mawanjiachen2021@mail.scut.edu.cn).

the MLMC method can be almost reduced to $O(\epsilon^{-5/2})$ for the risk estimation problem (1). We find that the main challenge is the special character of the indicator function $\mathbb{I}(\cdot < c)$, which prevents MLMC from achieving the optimal complexity of $O(\epsilon^{-2})$.

To address this difficulty, we consider to make indicator function $\mathbb{I}(\cdot < c)$ to a smooth function. In many work [15] [16], Fourier analysis has been successfully applied to pricing options. For example, Bakshi and Madam [15] used the characteristic function of the state-price density to analytically price options. Betas [16] successfully used the characteristic function to deal with Deutsche Mark options. We build upon the work of Jin and Zhang [17] to address the indicator function $\mathbb{I}(\cdot < c)$, which is a special Fourier transform method. The Fourier transform method not only alters the form of the indicator function but also renders it a smooth function. Through numerical studies, we find that the Fourier transform method significantly reduces the cost of MLMC for problem (1). Additionally, we discuss the influence of different truncation points on the varied Fourier transform integration. Next, in order to further enhance the efficiency of the MLMC method, we focus on using the quasi-Monte Carlo method. Compared to the Monte Carlo method, the QMC method uses more uniform point sequences, resulting in a smaller variance of the estimator. Details of QMC method details refer to Niederreiter [18]; Dick et al. [19]; L'Ecuyer and Lemieux [20]. In pioneering work by Giles and Waterhouse [21], a combination of the QMC method and the MLMC method was proposed. Recently, we have referred to some relevant work about the multilevel QMC method. Kuo et al. [22][23] used the multilevel QMC method to solve a class of elliptic partial differential equations (PDEs) and lognormal diffusion problems. Dick et al. [24] dealt with parametric operator equations, and Scheichl et al. [25] computed an inverse problem of uncertainty quantification, among other applications.

We use the randomized QMC (RQMC) method to replace the Monte Carlo method in the inner simulation stage. In simple terms, during the outer stage, we use the Monte Carlo simulation to produce a large number of Y samples, which represent all relevant risk factors.

In particularly, during the inner stage, we use the RQMC method to generate the corresponding X. This procedure is closely related to Giles and Haji-Ali's work [10], as well as Goda et al.'s work [13]. The former used a nested multilevel Monte Carlo estimator to address the beyond probability problem, while the latter used a nested multilevel RQMC estimator to solve the expected value of partial perfect information (EVPPI) problem.

The present work aims to improve the MLMC method for financial risk management by utilizing the Fourier transform method to tackle the indicator function. We successfully transform the discontinuous form of problem (1) and ensured that the new form of the Fourier transform function is sufficiently smooth, which yields favorable performance in numerical tests regarding the antithetic MLMC method. Furthermore, the potential benefits of employing an antithetic MLMC approach with RQMC to further enhance the efficiency of the Fourier transform method. Our numerical studies demonstrate that the Fourier transform multilevel quasi-Monte Carlo (FMLQMC) method exhibits a superior performance compared to the Fourier transform multilevel Monte Carlo (FMLMC) method, both of which converge towards an optimal complexity of $O(\epsilon^{-2})$. In Section 2, we review nested simulation and the MLMC method. After introducing the basic MLMC method, we develop an antithetic MLMC estimator for problem (1). The effects of the indicator function on nested simulation are discussed. In Section 3, we refer to the Fourier transform method and QMC method, with the former aimed at overcoming the discontinuity of the indicator function and the latter focused on reducing the variance of the MC estimator. In Section 4, we use some numerical experiments to test the validity of the Fourier transform method and RQMC method. Finally, we conclude this paper with some remarks in Section 5.

II. Nested simulation and Multilevel Monte Carlo

A. Nested Simulation

Our goal is to estimate the probability of future loss less than a given threshold c. As mentioned earlier, this probability can be computed using a nested simulation. In problem (1), we set $F(c) = \mathbb{E}[\mathbb{I}\{\triangle V \leq c\}]$. Frist, in the outer layer simulation, we produce N independent and identically distributed (i.i.d) copies of Y. Then we can get the

$$\hat{F}(c) = \frac{1}{N}\sum_{i=1}^{N}\mathbb{I}\{\triangle\hat{V}(Y_i) \leq c\}. \tag{4}$$

In the inner layer, we base Y_i to generate the corresponding X_j. Through (2), the future loss $\triangle V$ is determined by variables Y and X, where $\triangle\hat{V}(Y_i) = \mathbb{E}[X|Y_i]$. Thus, we can obtain the expression of the estimator:

$$\triangle\hat{V}_M(Y_i) = \frac{1}{M}\sum_{j=1}^{M}X_j(Y_i). \tag{5}$$

By substituting (5) for (4), the standard statistic in the nested simulation is given by:

$$\hat{F}_{N,M}(c) = \frac{1}{N}\sum_{i=1}^{N}\mathbb{I}\{\frac{1}{M}\sum_{j=1}^{M}X_j(Y_i) \leq c\}. \tag{6}$$

Specially, $\triangle V(Y_i) = \mathbb{E}[X|Y_i]$ is a conditional expectation. Referring to Broadie et al. [3], when using the standard Monte Carlo method to calculate the statistic, we need a sampling number of N that is $O(\epsilon^{-2})$ and a matching number of M that is $O(\epsilon^{-1})$, in order to achieve a root mean-squared error of ϵ. The total calculation cost is $N \times M = O(\epsilon^{-2}) \times O(\epsilon^{-1}) = O(\epsilon^{-3})$. Giles and Haji-Ali [10] proved that to estimate problem (1), the computational complexity is decreased to $O(\epsilon^{-2}|\log\epsilon|^2)$.

B. MLMC Estimators

In the subsection, we will follow the work of Giles and Haji-Ali [10] to briefly review the main concept of the MLMC method. Our target is to efficiently measure

$F(\triangle V) = \mathbb{E}[\mathbb{I}\{\triangle V \leq c\}]$. Let $P = \mathbb{I}\{\triangle V \leq c\}$ for a random output variable P, and every sample of P requires a finite cost to calculate. Unlike two-level standard Monte Carlo nested simulation, we do not directly evaluate P. Considering a sequence of random variables $P_0, P_1, \cdots$ with increasing approximation accuracy to P, and the computational cost also rises with the addition of subscripts in P. We define the ℓth level estimator of P is $P_\ell = \mathbb{I}\{\triangle \hat{V}_{m_\ell} \leq c\}$. In the inner simulation $\triangle \hat{V}_{m_\ell}$, we set $m_\ell = m_0^{\ell+\ell_0}$ with $m_0 = 2$ and $\ell_0 \geq 0$. By the linearity of expectation, we have

$$\mathbb{E}[P_L] = \mathbb{E}[P_0] + \sum_{\ell=0}^{L} \mathbb{E}[P_\ell - P_{\ell-1}]. \tag{7}$$

Assume a sequence of random variables $Z_\ell, \ell = 0, 1, \cdots$ which satisfies

$$\begin{cases} Z_0 &= P_0 = \mathbb{I}\{\triangle \hat{V}_{m_0} \leq c\} \qquad \text{if } \ell = 0, \\ Z_\ell &= P_\ell - P_{\ell-1} \\ &= \mathbb{I}\{\triangle \hat{V}_{m_\ell} \leq c\} - \mathbb{I}\{\triangle \hat{V}_{m_{\ell-1}} \leq c\} \qquad \text{if } \ell > 0. \end{cases}$$

For reducing the variance of Z_ℓ, we use a strategy [10]: using an antithetic form for coupling the consecutive levels, i.e.,

$$\begin{aligned} Z_\ell =& \mathbb{I}\{\triangle \hat{V}_{m_\ell}(Y) \leq c\} - \frac{1}{2}(\mathbb{I}\{\triangle \hat{V}^{(1)}_{m_{\ell-1}}(Y) \leq c\} \\ &+ \mathbb{I}\{\triangle \hat{V}^{(2)}_{m_{\ell-1}}(Y) \leq c\}), \end{aligned} \tag{8}$$

where

$$\triangle \hat{V}^{(i)}_{m_{\ell-1}}(Y) = \frac{1}{m_{\ell-1}} \sum_{j=1+(i-1)m_{\ell-1}}^{im_{\ell-1}} X_j(Y), \quad i = 1, 2.$$

By substituting Z_ℓ into (7), we have

$$\mathbb{E}[P_L] = \sum_{\ell=0}^{L} \mathbb{E}[Z_\ell]. \tag{9}$$

In the MLMC method, we independently estimate the right hand side of (9). Let $\hat{\mu}_\ell$ be the Monte Carlo estimator of $\mathbb{E}[Z_\ell]$ with N_ℓ samples:

$$\hat{\mu}_\ell = \frac{1}{N_\ell} \sum_{i=1}^{N_\ell} Z_\ell^{(i)}, \tag{10}$$

where $Z_\ell^{(1)}, \cdots, Z_\ell^{(N_\ell)}$ are i.i.d samples of Z_ℓ for $\ell = 0, \cdots, L$. The MLMC estimator is given by

$$\hat{F}_{MLMC} = \sum_{\ell=0}^{L} \hat{\mu}_\ell. \tag{11}$$

Denote the variance and the cost of Z_ℓ by V_ℓ and C_ℓ, respectively. We get the mean-squared error (MSE) of $\hat{F}_{MLMC}$:

$$\begin{aligned} \mathbb{E}[(\hat{F}_{MLMC} - \mathbb{E}[P])^2] =& \mathbb{E}[(\sum_{\ell=0}^{L} \hat{\mu}_\ell - \mathbb{E}[P])^2] \\ =& \sum_{\ell=0}^{L} \frac{V_\ell}{N_\ell} + \mathbb{E}[(P_L - P)^2]. \end{aligned} \tag{12}$$

In this case, the total cost of $\hat{F}_{MLMC}$ estimator is $C = \sum_{\ell=0}^{L} N_\ell C_\ell$.

By Giles [8], he proved the following complexity theorem for the MLMC method.

Theorem 1. *Suppose there are constants α, β, γ, c_1, c_2, c_3 such that $\alpha \geq min(\beta, \gamma)/2$ and*

- $|\mathbb{E}[P_\ell - P]| \leq c_1 m_\ell^{-\alpha}$,
- $\mathbb{E}[Z_\ell] = \begin{cases} \mathbb{E}[P_0] & \ell = 0, \\ \mathbb{E}[P_\ell - P_{\ell-1}] & \ell > 0. \end{cases}$
- $V_\ell \leq c_2 m_\ell^{-\beta}$,
- $C_\ell \leq c_3 m_\ell^{\gamma}$,

then there exists a constant $c_4 \geq 0$ such that for any $\epsilon < 1/e$, there are value L and N_ℓ for which the MLMC estimator $\hat{F}_{MLMC}$ has a mean square error bound $\mathbb{E}[(\hat{F}_{MLMC} - P)^2] \leq \epsilon^2$ with a total computational cost C with bound

$$C = \begin{cases} c_4 \varepsilon^{-2}, & \beta > \gamma \\ c_4 \varepsilon^{-2} (\log \varepsilon)^2, & \beta = \gamma \\ c_4 \varepsilon^{-2-(\gamma-\beta)/\alpha}, & \beta < \gamma. \end{cases} \tag{13}$$

In Theorem 1, the constant α represents the bias decreasing rate, commonly refer as *weak convergence*. The constant β describes the variance decreasing rate and is generally known as *strong convergence*. Finally, the constant γ controls the increasing rate of computing budget for each sample. We try to make the estimator $\hat{F}_{MLMC}$ in the $O(\epsilon^{-2})$ regime as much as possible, with $\beta > \gamma$. In the risk estimation problem (1), the computational complexity of the antithetic MLMC method is $O(\epsilon^{-5/2})$, which was proved by Giles and Haji-Ali [11]. In order to reduce the total cost of antithetic MLMC about problem (1), we will introduce a Fourier transform method and quasi-Monte Carlo method in the next section.

III. Fourier transform method and quasi-Monte Carlo method

A. Traditional Option Transform Method

Fourier analysis is successfully employed to price individual options. If the characteristic function $\phi_T(u)$ of the stock return process is known, then the price of an European call option is

$$C = S\Pi_1 - Ke^{-rT}\Pi_2,$$

where Π_2 is the risk-neutral in-the-money probability in the form of Fourier inversion

$$\begin{aligned} \Pi_2 &= Pr(S_T > K) \\ &= \frac{1}{2} + \frac{1}{\pi} \int_o^\infty Re(\frac{e^{-iu\ln(K)}\phi_T(u)}{iu}) \mathrm{d}u, \end{aligned} \tag{14}$$

and Π_1 is the delta of the option determined through

$$\Pi_1 = \frac{1}{2} + \frac{1}{\pi} \int_0^\infty Re(\frac{e^{-iu\ln(K)}\phi_T(u-i)}{iu\phi_T(-i)}) \mathrm{d}u, \tag{15}$$

$Re(x)$ is the real part of complex number x. Indeed, the traditional Fourier analysis method has some flaws:

- In generally, we cannot obtain the characteristic function of the portfolio value change analytically.
- Supposing we have the characteristic function, it is not straightforward to transform (14) and (15).
- The integrand of the traditional approach [15] [16] is highly oscillating around zero.

B. Fourier Transform Method

Different from the traditional methods [15] [16], we focus on simulating the evolution of portfolio value. The Fourier transform utilizes the distribution function related to (1) to obtain:

$$F(c) = \frac{1}{2} - \frac{1}{\pi}\int_0^{\infty} \mathbb{E}[Re(\frac{e^{iu(\triangle V - c)}}{iu})]\mathrm{d}u. \quad (16)$$

And approximating the integral:

$$\int_0^{\infty} \mathbb{E}[Re(\frac{e^{iu(\triangle V - c)}}{iu})]\mathrm{d}u \approx \int_0^{T} \mathbb{E}[Re(\frac{e^{iu(\triangle V - c)}}{iu})]\mathrm{d}u, \quad (17)$$

for a suitable chosen T, which is truncation point about the integration. Each $S_i(t)$ is assumed to be equal to a smooth function of a Brownian motion, and the geometric Brownian motion is smooth with respect to a uniform random variable, which results in the integrand $Re(\frac{e^{iu(\triangle V - c)}}{iu})$ being smooth on $[0, 1]^{d+1}$.

It is noteworthy that the selection of truncation point T is critical. Jin and Zhang [17] proposed an algorithm for selecting T. Generally, we select $T = 2$, which is sufficient for a wide range of functions. To estimate the distribution function $F(c)$, we use the following simulation-based estimator:

$$\hat{F}_{T,n}(c) = \frac{1}{2} - \frac{T}{\pi}\frac{1}{n}\sum_{i=1}^{n}[Re\frac{e^{it_i(\triangle V_i - c)}}{it_i}], \quad (18)$$

where t_i is a sampling from the interval $[0, T]$, and $\triangle V_i$ is a sampling of the portfolio value change.

Next, Jin and Zhang [17] developed an alternative approach to estimate $F(c)$ via Fourier transform. Consider the Fourier transformation of $e^{-kc}F(c)$ to replace $F(c)$, where $k > 0$,

$$f(t) = \int_{-\infty}^{+\infty} e^{-kc}F(c)e^{-i2\pi tc}\mathrm{d}c \quad (19)$$

We assume that $e^{-kc}F(c)$ is integrable over $(-\infty, +\infty)$ and

$$\lim_{c\to-\infty} e^{-kc}F(c) = 0, \quad k \geq k_0,$$

for some $k_0 > 0$. Applying integration by parts yields that

$$f(t) = \int_{-\infty}^{+\infty} \frac{e^{-(k+i2\pi t)c}}{k + i2\pi t}\mathrm{d}F(c) = \frac{\mathbb{E}[e^{-(k+i2\pi t)\triangle V}]}{k + i2\pi t}.$$

Assume that $F(c)$ is continuous at c. Inverting the preceding function (1) yields that

$$\begin{aligned} F(c) &= \int_{-\infty}^{+\infty} e^{kc}f(t)e^{i2\pi tc}\mathrm{d}t \\ &= \int_{-\infty}^{+\infty} e^{kc}\frac{\mathbb{E}[e^{-(k+i2\pi t)\triangle V}]}{k + i2\pi t}e^{i2\pi tc}\mathrm{d}t \\ &= \int_0^{+\infty} \frac{2}{k^2 + (2\pi t)^2}\mathbb{E}[e^{k(c-\triangle V)}(k\cos(2\pi t(c - \triangle V)) \\ &\quad + 2\pi t\sin(2\pi t(c - \triangle V)))]\mathrm{d}t. \end{aligned} \quad (20)$$

By the (3), ξ_α is determined by the demand of risk management at the function $F(c)$ in this paper. Jin and Zhang [17] proposed a method to normalize $\triangle V - c$ as follows:

$$\begin{aligned} F(c) &\equiv \mathbb{P}[\frac{\triangle V - c}{\xi_\alpha} \leq 0] \\ &= \int_0^{+\infty} \frac{2}{k^2 + (2\pi t)^2}\mathbb{E}[e^{kV_c}(k\cos(2\pi tV_c) \\ &\quad + 2\pi t\sin(2\pi tV_c))]\mathrm{d}t, \end{aligned} \quad (21)$$

where

$$V_c = \frac{c - \triangle V}{\xi_\alpha}.$$

In the Fourier transform form, if k is a larger value, then the variance of the random variable e^{kV_c} is also larger, which results in larger variances of the estimator. Supposing k is smaller, although it leads to a reduction in the variance of the estimator, it also results in a larger truncation point, which causes $t/k^2 + (2\pi t)^2$ to converge more slowly to zero for smaller k. Referring the work of Jin and Zhang [17], $k = 2$ is a good choose in terms of the above work. Now function $F(c)$ becomes

$$\begin{aligned} F(c) = \int_0^{+\infty} \frac{1}{1 + \pi^2 t^2}\mathbb{E}[e^{2V_x}(\cos(2\pi tV_x) \\ + \pi t\sin(2\pi tV_x))]\mathrm{d}t. \end{aligned} \quad (22)$$

Nevertheless, the function (22) does not possess a closed-form expression. Thus, finding a method to approximate the function $F(c)$ directly is a viable approach. To this end, rewriting (22), we have

$$\begin{aligned} F(c) = \int_0^{+\infty} \frac{1}{1 + \pi^2 t^2}\{&\mathbb{E}[e^{2V_c}\cos(2\pi t\tilde{V})] \\ &\times (\cos(2\pi t) - \pi t\sin(2\pi t)) \\ &- \mathbb{E}[e^{2V_c}\sin(2\pi t\tilde{V})] \\ &\times (\sin(2\pi t) + \pi t\sin(2\pi t))\}\mathrm{d}t. \end{aligned} \quad (23)$$

where $\tilde{V} = \triangle V/\xi_\alpha$ and ξ_α is defined by (3). Now, we approximate $F(c)$ by

$$\begin{aligned} F_T(c) = \int_0^{T} \frac{1}{1 + \pi^2 t^2}\{&\mathbb{E}[e^{2V_c}\cos(2\pi t\tilde{V})] \\ &\times (\cos(2\pi t) - \pi t\sin(2\pi t)) \\ &- \mathbb{E}[e^{2V_c}\sin(2\pi t\tilde{V})] \\ &\times (\sin(2\pi t) + \pi t\sin(2\pi t))\}\mathrm{d}t, \end{aligned} \quad (24)$$

which $T > 0$ is a truncation point. For any fixed truncation error ϵ, the problem of truncating integral (23) is to find a point T_ϵ such that

$$|F_{T_\epsilon}(c) - F(c)| = |\tilde{F}_{T_\epsilon}(c)| \leq \epsilon, \quad (25)$$

where $\tilde{F}_{T_\epsilon}(c)$ is the remainder integral and is defined by

$$\begin{aligned} \tilde{F}_{T_\epsilon}(c) = \int_{T_\epsilon}^{+\infty} \frac{1}{1 + \pi^2 t^2}\{&\mathbb{E}[e^{2V_c}\cos(2\pi t\tilde{V})] \\ &\times (\cos(2\pi t) - \pi t\sin(2\pi t)) \\ &- \mathbb{E}[e^{2V_c}\sin(2\pi t\tilde{V})] \\ &\times (\sin(2\pi t) + \pi t\sin(2\pi t))\}\mathrm{d}t. \end{aligned} \quad (26)$$

To satisfy (25), Jin and Zhang [17] proved that $|\tilde{F}_{T_\epsilon}(c)| \leq \epsilon$ for $T \geq T_\epsilon$.

In the next, rewriting (24):

$$F_T(c) = \int_0^T \frac{1}{1+\pi^2 t^2}\mathbb{E}[e^{2V_c} \times (\cos(2\pi t V_c) + \pi t \sin(2\pi t V_c))]\mathrm{d}t. \quad (27)$$

The inner expectation is

$$g(\triangle V) = e^{2V_c}(\cos(2\pi t V_c) + \pi t \sin(2\pi t V_c)). \quad (28)$$

Because the function $g(\triangle V)$ is a smooth function, the complexity of MLMC is expected to be $O(\varepsilon^{-2})$. In section IV, we perform numerical study to verify this point.

C. Quasi-Monte Carlo Method

In this work, we use the quasi-Monte Carlo method to replace the Monte Carlo method within the random variables Z_ℓ, resulting in a multilevel quasi-Monte Carlo (MLQMC) estimator.

When we want to approximate the integrals of function, which is defined over the multi-dimensional unit cube $[0,1)^d$

$$I(\mathbf{u}) = \int_{[0,1)^d} h(\mathbf{u})\mathrm{d}\mathbf{u},$$

and choose M points set: $\{\mathbf{u}_1, \cdots, \mathbf{u}_M\}$. We approximate $I(\mathbf{u})$ by:

$$\hat{I}_M(\mathbf{u}) = \frac{1}{M}\sum_{j=1}^{M} h(\mathbf{u}_j),$$

where the Monte Carlo method was the random points set. However, QMC methods generate low discrepancy point sequences that are deterministically chosen from $[0,1)^d$ and are more uniformly distributed than randomly chosen uniform points. QMC methods have two main families of point sets: (t,d)-sequence [18] and lattice rules [26]. In this paper, we use the former with the antithetic MLMC estimator.

In our model, we assume that given $Y_i = y$, X can be generated by

$$X(y) = \varphi(\mathbf{u}; y). \quad (29)$$

In the situation, the inner estimator (5) is substituted by

$$\triangle\hat{V}_{m_\ell}(y) = \frac{1}{m_\ell}\sum_{j=1}^{m_\ell} \varphi(\mathbf{u}_j; y). \quad (30)$$

Now, by combining MLMC and QMC, we have

$$Z_\ell = \mathbb{I}\{\triangle\hat{V}_{m_\ell}(Y) \le c\} - \frac{1}{2}\mathbb{I}\{\triangle\hat{V}^{(1)}_{m_{\ell-1}}(Y) \le c\} - \frac{1}{2}\mathbb{I}\{\triangle\hat{V}^{(2)}_{m_{\ell-1}}(Y) \le c\}, \quad (31)$$

where

$$\triangle\hat{V}^{(i)}_{m_{\ell-1}}(Y) = \frac{1}{m_{\ell-1}}\sum_{j=1+(i-1)m_{\ell-1}}^{im_{\ell-1}} \varphi(\mathbf{u}_j; y), \quad i = 1, 2.$$

In the work of Goda et al. [13] and Giles and Goda's work [12], they demonstrated that antithetic sampling can significantly reduce variance. However, when dealing with a discontinuous function, the antithetic sampling method should be used with caution. It is essential that the equation

$$\mathbb{P}[\{\triangle\hat{V}^{(1)}_{m_{\ell-1}}(Y) \le c\}|Y] = \mathbb{P}[\{\triangle\hat{V}^{(2)}_{m_{\ell-1}}(Y) \le c\}|Y]$$

is used to ensure the telescoping representation (7) under the RQMC scheme. We note that the left half RQMC points $\mathbf{u}_1, \cdots, \mathbf{u}_{m_{\ell-1}}$ have the same joint distribution as the joint distribution of the right half RQMC points $\mathbf{u}_{m_{\ell-1}+1}, \cdots, \mathbf{u}_{m_\ell}$ in the point sequence selection.

In this paper, we use Owen's scrambling method (Owen [27]) to construct (t,d)-sequence in base $b = 2$, which have low discrepancy points. The RQMC method reduces the variance of the estimator, which enhances the efficiency of Fourier transform method. The effectiveness of the RQMC method will be demonstrated in the next section IV.

IV. Numerical study

In this study, we present numerical results that demonstrate the advantage of using the Fourier transform method in portfolio management. Specifically, our focus is on an European option portfolio comprising d stocks whose price dynamics follow a geometric Brownian motion process. The Fourier transform proves to be highly effective in capturing the underlying patterns and trends in stock prices, thereby facilitating informed investment decision-making. For simplicity, we assume that stock return are the same, denoted by μ, and risk-free interest rate is r. Price dynamics of the stocks $S_t = (S_t^1, S_t^2, \cdots, S_t^d)$ written according to

$$\frac{\mathrm{d}S_t^i}{S_t^i} = \mu^{'}\mathrm{d}t + \sum_{j=1}^{d}\sigma_{ij}\mathrm{d}W_t^i, \quad i = 1, 2, \cdots, d$$

where $\mu^{'} = \mu$ under the real-world probability measure $\mathbb{P}$, and $\mu^{'} = r$ under the risk-neutral probability measure $\mathbb{Q}$. Let $\mathbf{W}_t = (W_t^1, W_t^2, \cdots, W_t^d)$ denote a standard d-dimensional geometric Brownian motion which represents d risk factors in the portfolio model. Let $\mathbf{S}_0 = (S_0^1, S_0^2, \cdots, S_0^n)$ are the initial prices of stocks. By the Black-Scholes model, we have

$$S_t^i = S_0^i \exp\{(\mu^{'} - \frac{1}{2}\sum_{j=1}^{d}\sigma_{ij}^2)t + \sum_{j=1}^{d}\sigma_{ij}W_t^i\}, i = 1, 2, \cdots, d,$$

T denotes the maturities, which are the same for all the European options in the portfolio. In many financial applications, researchers are interested in measuring the portfolio risk at a future time $\tau (\tau < T)$. In the simulation, we firstly simulate the random variable $Y = \mathbf{S}_\tau = (S_\tau^1, S_\tau^2, \cdots,)$ under the real-world probability measure $\mathbb{P}$, which means that at the risk horizon τ the stocks prices as the outer sample. Based on the given value of Y, we simulate the inner samples in the next step, i.e. $\mathbf{S}_T = (S_T^1, S_T^2, \cdots, S_T^d)$ under the risk-neutral probability measure $\mathbb{Q}$ which is stocks prices at maturity. We use $V_0 = \sum_{i=1}^{d} v_0^i$ to denote the initial value of the portfolio, where every v_0^i is known by the Black-Scholes formula(Hull [28]). Then the portfolio value revenue is

$$\triangle V := V_0 - \mathbb{E}[V_T(\mathbf{S}_T)|Y], \quad (32)$$

where $V_T(\mathbf{S}_T)$ is the discounted payoff of the portfolio to initial time 0 at maturity time T, thus V_T is a function of $\mathbf{S}_T$.

Our objective is to gain the probability: $F(c) = \mathbb{P}[\triangle V < c]$, for a given threshold value c. Next, we will compare various methods, including MLMC, FMLMC, and FMLQMC, in each example.

A. Single Asset

In this initial instance, we will focus on a put option scenario where the portfolio consists of a single option, i.e. $d = 1$. This example was previously investigated by Broadie et al. [3].

The underlying asset follows a geometric Brownian motion with an initial price of $S_0 = 100$. The drift of this process under the real-world distribution used in the outer stage of simulation is $\mu = 8\%$. The annualized volatility is $\sigma = 20\%$. The risk-free rate is $r = 3\%$. The strike of the put option is $K = 95$, and the maturity is $T = 0.25$ years (i.e., three months). The risk horizon is $\tau = 1/52$ years (i.e., one week). With these parameters, the initial value of the put option is $v_0 = 1.6691$ which given by the Black–Scholes formula.

In the simulation, the outer random variable is generated by

$$Y := S_\tau = S_0 \exp\{(\mu - \sigma^2/2)\tau + \sigma\sqrt{\tau}Z\}, \tag{33}$$

where the real-valued risk factor Z is a standard normal random variable. The portfolio value change is

$$\triangle V = V_0 - \mathbb{E}[e^{-r(T-\tau)}(K - S_T(Y,W))^+|Y], \tag{34}$$

where the expectation is taken over the random variable W, which is a standard normal random variable independent with Z, and $S_T(Y,W)$ is given by

$$S_T(Y,W) = Y \exp\{(r - \sigma^2/2)(T-\tau) + \sigma\sqrt{T-\tau}W\}. \tag{35}$$

Notice that outer stage scenarios are generated using the real-world distribution governed by the drift μ, while inner stage scenarios used to generate future put option prices are generated using the risk-neutral distribution governed by the drift r.

Now let $X = v_0 - e^{-r(T-\tau)}(K - S_T(Y,W))^+$. For a given value of $Y = y$ and combined with (35), X can be generated by

$$\begin{aligned} X(y) =& \varphi(u;y) \\ =& v_0 - e^{-r(T-\tau)}(K - y\exp\{(r-\sigma^2/2)(T-\tau) \\ &+ \sigma\sqrt{T-\tau}\Phi^{-1}(u)\})^+. \end{aligned} \tag{36}$$

where $W = \Phi^{-1}(u)$. In the inner simulation, we use scrambling $(t,1)$-sequence in base $b = 2$.

By the definition of (34), we have $\triangle V = \mathbb{E}[X|Y]$. For this example, the VaR is given by (3), and Theorem 1 shows that $F(c)$ is a strictly increasing continuous function. Therefore, the cumulative function of $\triangle V(Y)$ can be computed easily, namely,

$$\begin{aligned} &\mathbb{P}[\triangle V(Y) \le c] \\ &= \mathbb{P}\{V_0 - \mathbb{E}[e^{-r(T-\tau)}(K - S_T(Y,W))^+] \le c\} \\ &= \mathbb{P}\{\int_0^T \frac{1}{1+\pi^2 t^2}\mathbb{E}[e^{2V_x}(\cos(2\pi t V_x) \\ &\qquad + \pi t \sin(2\pi t V_x))]\mathrm{d}t \le c\}. \end{aligned} \tag{37}$$

We choose $c = -\xi_\alpha = -0.859$ to correspond to the loss probability α of 10% which is computed explicitly using the Black-Scholes formula. In the context of this single asset problem, we employ the Fourier transform MLMC and Fourier transform MLQMC methods with a truncation point $T = 2$. The results on testing the weak convergence and the strong convergence in Figure 1 are based on $200,000$ outer samples at each level, and we set the error bound to be $\epsilon = 0.05$.

In the case of $\epsilon = 0.05$ and $\ell = 6$, the test result of the FMLQMC method achieved an MSE error bound equivalent to that of the FMLMC method and the MLMC method, which had a lower level of $\ell = 10$. In other words, FMLQMC method achieved the desired accuracy requirement with only half of the number of levels. Fig 1(a) displays the weak convergence rate of three methods, with FMLQMC method having the largest weak convergence α which is twice as fast as that of FMLMC and MLMC methods. When the level $\ell \ge 6$, there is no significant difference between the mean numerical results obtained by FMLMC and MLMC methods, indicating that the Fourier transform method does not affect the weak convergence and numerical result in MLMC method. In comparison to the other two methods, the FMLQMC method exhibits the least absolute value at finest level, highlighting its superiority.

Fig 1(b) shows the comparison of strong convergence, which is a crucial aspect in the methodology of MLMC method. In the picture, although the variance of FMLQMC and FMLMC methods at the initial hierarchy level is significantly larger than that of method MLMC, when the level $\ell \ge 5$, the variance of FMLQMC is lower than that of MLMC; and when $\ell \ge 8$ the variance of FMLMC is lower than that of MLMC. The outcome implies that Fourier transform MLMC methods outperform MLMC method.

Based on the Theorem 1, we can know the three different computational cost of MLMC method. For the sake of simplification, in the work of Giles [8], he fixed $\gamma = 1$ in the MLMC method, then the three costs situation is based the β value. In order to facilitate a clearer comparison, we have superimposed three distinct dashed lines at a specific node in each scenario, highlighting the downward trend observed under varying values of β. In the FMLQMC case, we set a specific node at $\ell = 2$ and theoretically plotted the downward trend of $\beta = 2$. It is evident from our observations that the variance at level 6 is considerably lower than the theoretical value of $\beta = 2$. Therefore, through comparison, we can conclude that FMLQMC method has strong convergence parameter $\beta_{FMLMQMC}$ value greater than 2. In the FMLMC case, through a similar comparison for FMLQMC, we can determine that FMLMC method has β_{FMLMC} value

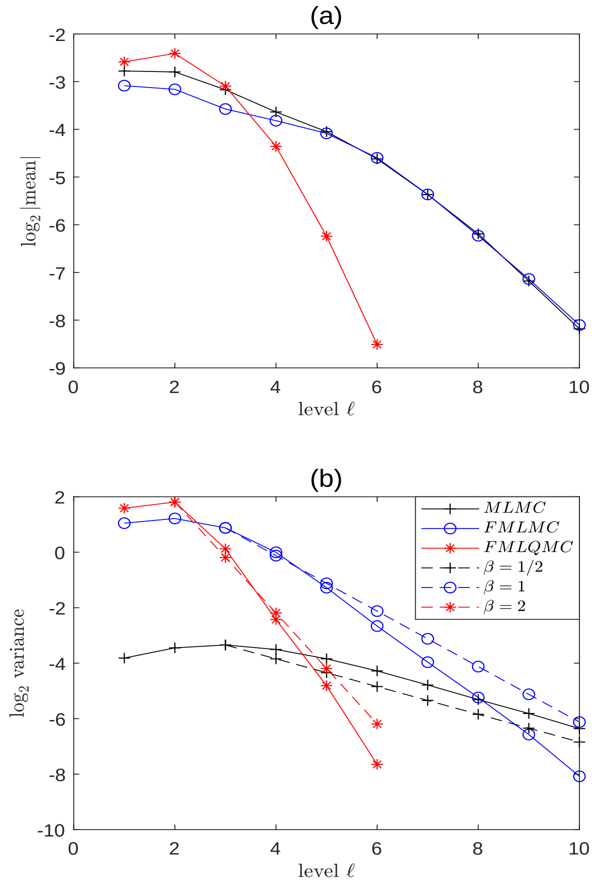

Fig. 1. The Mean and Variance Comparison of MLMC, FMLMC, FMLQMC for the Single Asset Case

larger than 1. In MLMC case, we can see that the plot has same decline rate for $\beta = 1/2$, which means β_{MLMC} is nearly equal to 1/2.

Consequently, Fourier transform MLMC methods lead $\beta > \gamma = 1$, indicating a faster decrease rate for variance V_ℓ than an increasing rate for cost C_ℓ. Based on the fundamental principle of MLMC method, in this case, we can achieve the goal of reducing computational cost. Furthermore, QMC method is capable of further reducing the variance and improving the strong convergence rate. Additionally, the FMLMC method exhibits a sample size reduction rate identical to that of the FMLQMC method, leading to a lower variance. As a result, the costs for each level are reduced accordingly, as demonstrated by Fig 2.

In Fig 2, we display each level $N_\ell, \ell = 0, 1, 2, \cdots$ under three different scenarios. In Fig 2(a), the MSE error bound is $\epsilon = 5 \times 10^{-3}$. The FMLQMC method employs $\ell = 7$ levels, the MLMC method uses $\ell = 12$ levels and the FMLMC method employs $\ell = 14$ levels. It is evident that the decline rate of FMLQMC method is the fastest, while the antithetic MLMC method exhibits the slowest decline rate. Although the levels of FMLMC is bigger than MLMC, but comparison the computational cost, the cost of MLMC is gigger than FMLMC cost. This observation further supports the validity of strong convergence through other aspects. Fig 2(b) and Fig

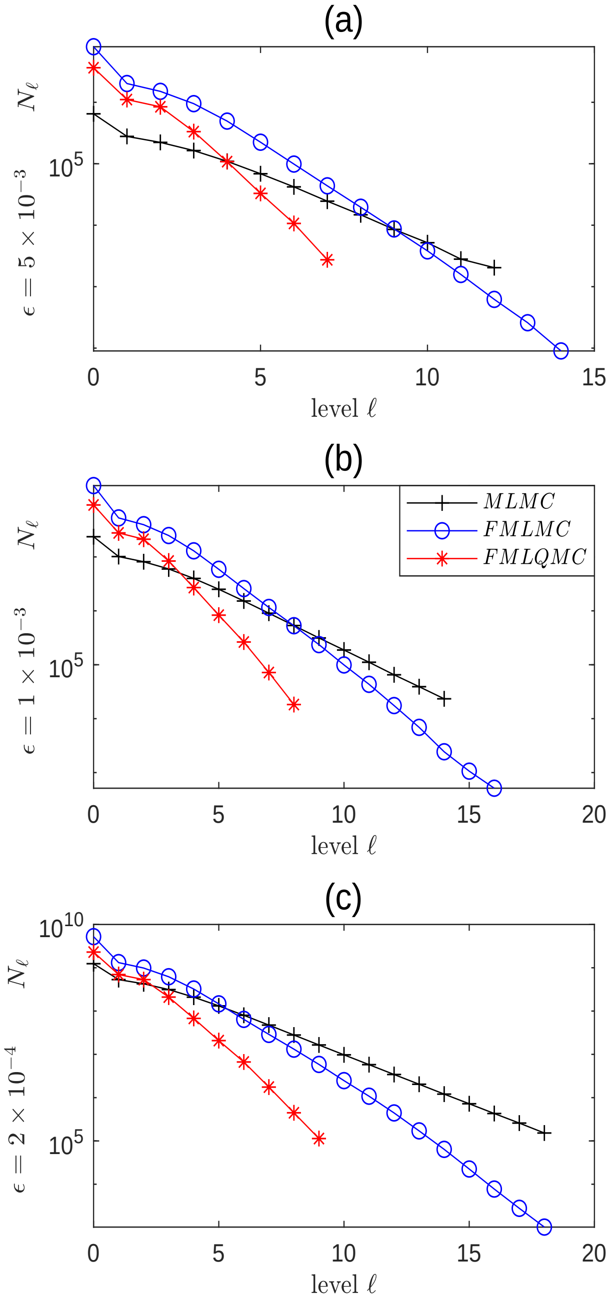

Fig. 2. N_ℓ Comparison of MLMC,FMLMC,FMLQMC for the Single Asset Case

2(c) exhibit the same phenomenon as Fig 2(a), which is once again consistent with Theorem 1. As the accuracy demand increases, the rate at which the level L of MLMC increases is faster than that of FMLMC and FMLQMC. This indicates that the behaviors of FMLMC and FMLQMC are superior to that of MLMC.

As previously mentioned, FMLMC methods can accelerate strong convergence, resulting in $\beta > \gamma = 1$ in Theorem 1. In our numerical experiment, we calculate the $\beta_{FMLQMC} = 1.96$ and $\beta_{FMLMC} = 1.34$. Then the total cost falls in $\beta > \gamma$ situation in Theorem 1,

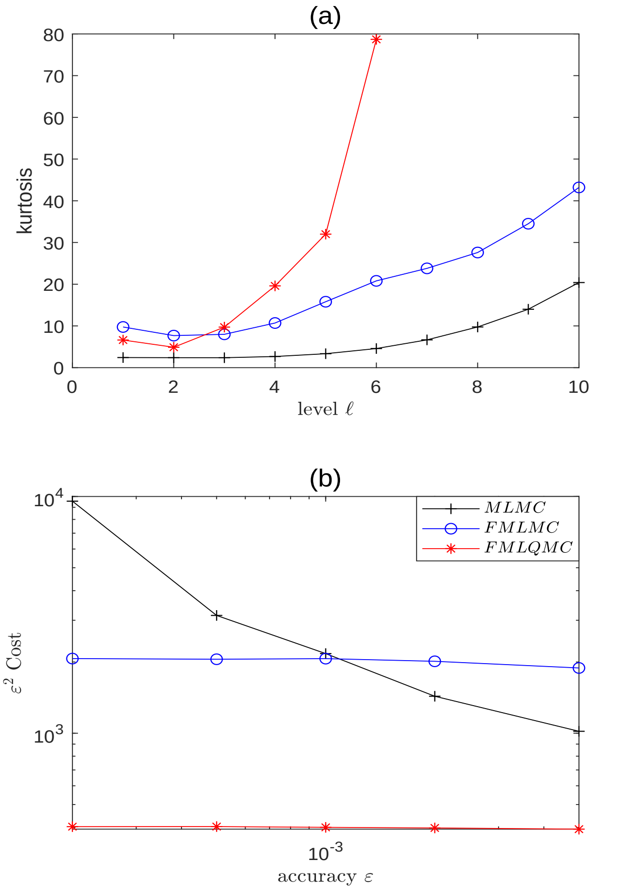

Fig. 3. the Kurtosis and Cost Comparison of MLMC, FMLMC, FMLQMC

which is the optimal complexity $O(\epsilon^2)$. When we want to achieve the high accuracy demand, there is no doubt that the efficiency of using FMLMC methods optimal the antithetic MLMC method. Fig 3(b) confirms this with numerical results. The FMLMC methods perform the best in terms of complexity, whereas the FMLQMC method reduces the computational burden.

Fig 3(a) illustrates the trend of kurtosis. As previously stated, kurtosis increases as variance decreases and ℓ grows. The special structure of the indicator function causes this phenomenon to occur, but when combined with Fourier transform MLMC method, the increase in kurtosis slows down significantly, indicating that Fourier transform MLQMC method affects the occurrence of high-kurtosis phenomenon. In other part, when the variance of a random variable is small, its kurtosis tends to increase. Fortunately, the high-kurtosis phenomenon does not affect the effectiveness of the MLMC method and the validity of random sampling.

B. Multiple Asset

Now we consider a portfolio consisting of d European call options, which was studied in Hong et al. [7]. Given the outer sample $Y = \mathbf{S}_\tau = (S_\tau^1, S_\tau^2, \cdots, S_\tau^d)$, the price of stocks at the risk horizon τ under real-world measure, and $\mathbf{K} = (K^1, K^2, \cdots, K^d)$, the strike price for call options. The portfolio value change is

$$\triangle V = V_0 - \mathbb{E}[e^{-r(T-\tau)} \sum_{i=1}^{d} (S_T^i(Y^i, W) - K^i)^+ | Y], \tag{38}$$

where Y^i is the ith element of the vector Y and the expectation is taken over the random variable $\mathbf{W} = (W^1, W^2, \cdots, W^d) \sim N(\mathbf{0}, \mathbf{I}_d)$, and samples of

$$S_T^i(Y^i, \mathbf{W}) = Y^i \exp\{(r - \frac{1}{2}\sum_{j=1}^{d} \sigma_{ij}^2)(T-\tau) + \sum_{j=1}^{d} \sigma_{ij}\sqrt{T-\tau}W^j\} \tag{39}$$

are simulated under the risk-neutral measure.

The parameters in our experiments are set as follows: $S_0^1 = S_0^2 = \cdots = S_0^d$, $\mu = 8\%$, $r = 5\%$, the strikes $K^1 = K^2 = \cdots = K^d = 95$, the maturity $T = 0.1$, and the risk horizon $\tau = 0.02$. Without loss of generality, we let $\sum = (\sigma_{ij})$ be a sub-triangular matrix satisfying $C = \sum \sum^T$ which corresponds with Cholesky decomposition of C, where $C_{ij} = 0.3^2 \cdot 0.98^{|i-j|}$. It is worth noting that the distinct decompositions of C do not impact the efficiency of the MC method, but they do influence the performance under QMC scheme. The Cholesky decomposition, on the other hand, is a common and standard approach in QMC simulations. We set the threshold $c = 50\% V_0$ and take truncation point $T = 2$ in the Fourier transform MLMC and Fourier transform MLQMC methods. Given the absence of analytical solutions for portfolios involving multiple assets, we resort to the conventional nested method to obtain data points for this illustration. Moving forward, we will compare the performance of the MLMC, FMLMC and FMLQMC methods.

To begin with, we perform the convergence tests for estimating parameter α and β in Theorem 1. The results are based on 200,000 outer samples at each level. Fig 4(a) shows the behavior of the absolute value for the expectation of Z_ℓ for the crude method and $\tilde{Z}_\ell$ for the smoothed methods. It is evident that the smoothed method attains the same level of convergence precision as the smaller value, yet converges more rapidly. The absolute mean values calculated by the FMLMC method and MLMC method are nearly identical, suggesting that the FMLMC method introduces minimal errors and substantiating the viability of employing the Fourier transform method. Comparing with FMLMC and MLMC methods, we can observe that FMLQMC method achieves the desired accuracy with only half the number of levels. Contrary to the single-asset model, the FMLQMC method demonstrates a faster convergence rate compared to other methods when addressing multi-dimensional issues. The next Fig 4(b) illustrates the variances of the three methods, which can be utilized to predict the strong convergence rate β through ordinary linear regression.

The FMLQMC method has the fastest declining rate, followed by FMLMC method, and then MLMC method.

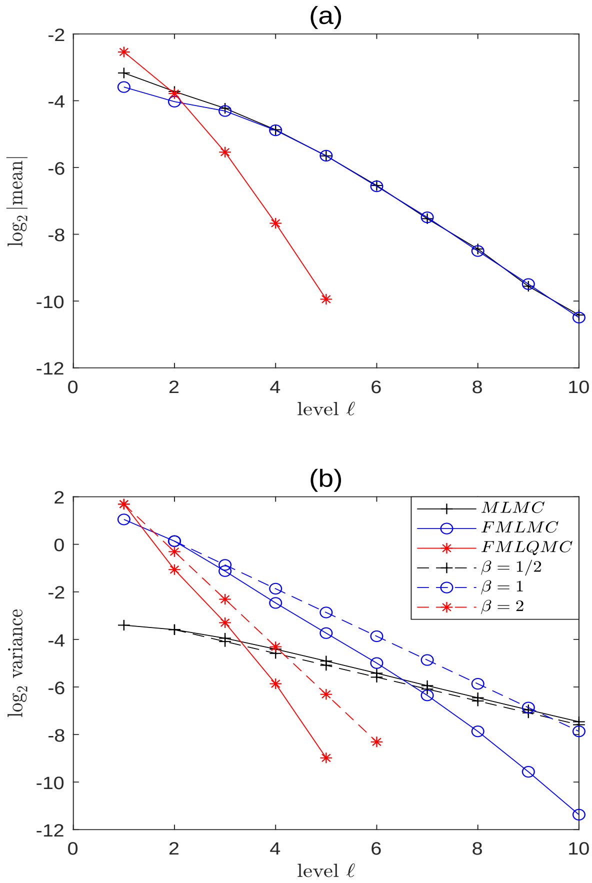

Fig. 4. Estimations of $|\mathbb{E}Z_\ell|$ and $\mathrm{Var}(Z_\ell)$

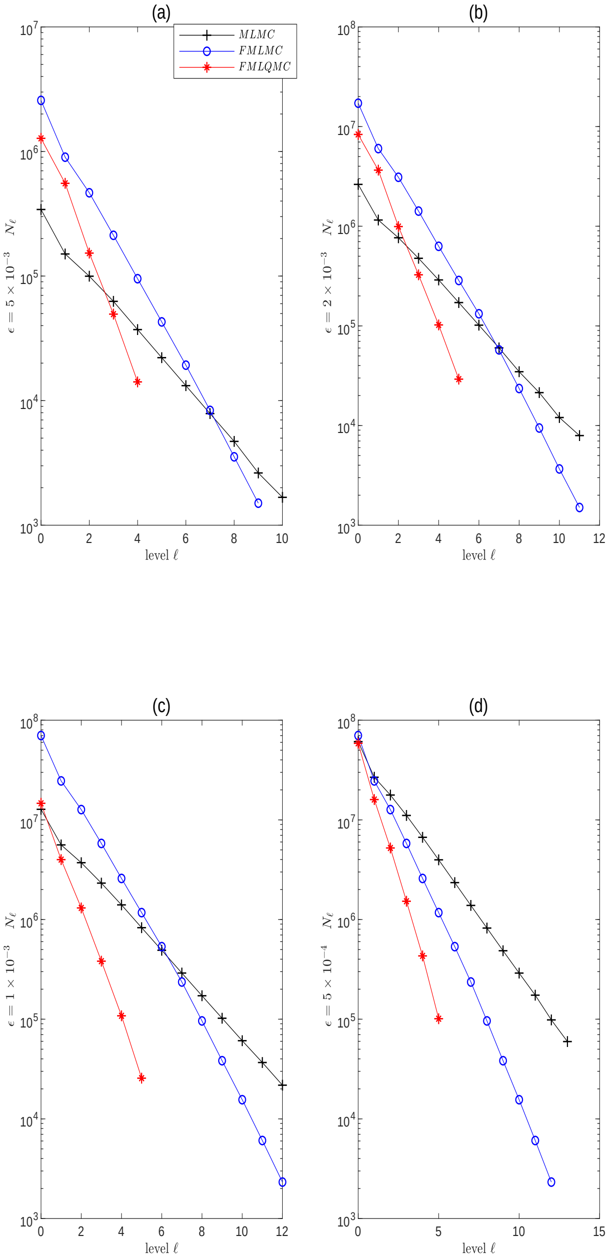

Fig. 5. N_ℓ Comparison of Multiple Asset Case

To clearly illustrate the potential effects of the slope of parameter β, we plotted dashed lines with different slopes which illustrate some case for β value. Firstly, the case of FMLQMC corresponds to parameter $\beta = 2$. It is obvious that the β value of FMLQMC is exceeding 2. It is noteworthy that the strong convergence rate of FMLMC method exhibits better performance in 5-dimensional scenarios compared to its counterpart in low-dimensional case. Secondly, the cases of methods FMLMC and MLMC correspond to parameters $\beta = 1$ and $\beta = 0.5$, respectively. Finally, in order to make the comparison more significant, we calculated the numerical values of parameter β corresponding to different methods through numerical calculations. We obtain that $\beta_{FMLQMC} = 2.61$ and $\beta_{FMLMC} = 1.47$ in the 5-dimension scenario using numerical calculation. For the plain MLMC, we observe $\beta_{MLMC} \approx 0.5$. The strong convergence get apparent improvement with Fourier transform methods, in which $\beta > \gamma = 1$. For smoothed methods, these complexity is $O(\varepsilon^{-2})$. In higher ℓ level, Fourier transform MLMC methods achieve smaller variance and reduce costs accordingly, as evidenced by Fig 5.

In Fig 5, we depict the sampling size at each level for four error demand scenarios. As demand for accuracy increases, the value of N_ℓ for the same level also increases. For example, when $\epsilon = 5 \times 10^{-3}$, FMLMC method requires $N_0 \approx 10^6$; when $\epsilon = 1 \times 10^{-3}$, FMLMC method requires $N_0 \approx 10^8$. Although the initial level sampling of MLMC method is larger than that of FMLMC method, at higher levels, the number of samples sampled by FMLMC method is obviously smaller than that of MLMC method. When the error bound is the same, Fourier transform method enhances the declining rate of N_ℓ numbers. Similar to the case of $d = 1$, as ℓ increases, the kurtosis also grows larger, as shown in Fig 6(a). It is worth noting that QMC method leads to a very small variance, which inevitably causes the high kurtosis phenomenon. Fortunately, FMLQMC method

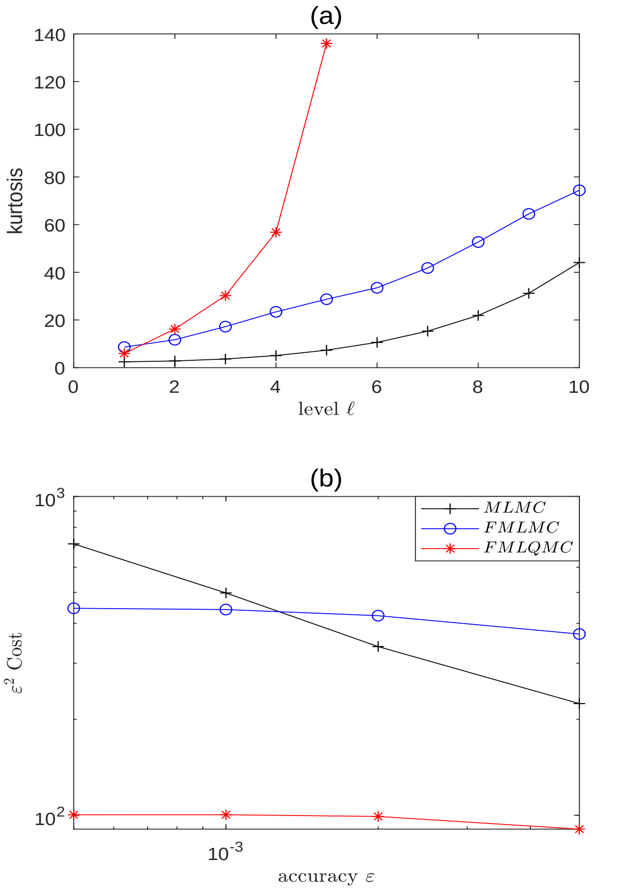

Fig. 6. Tests of Kurtosis and Total Cost about Multiple Assets

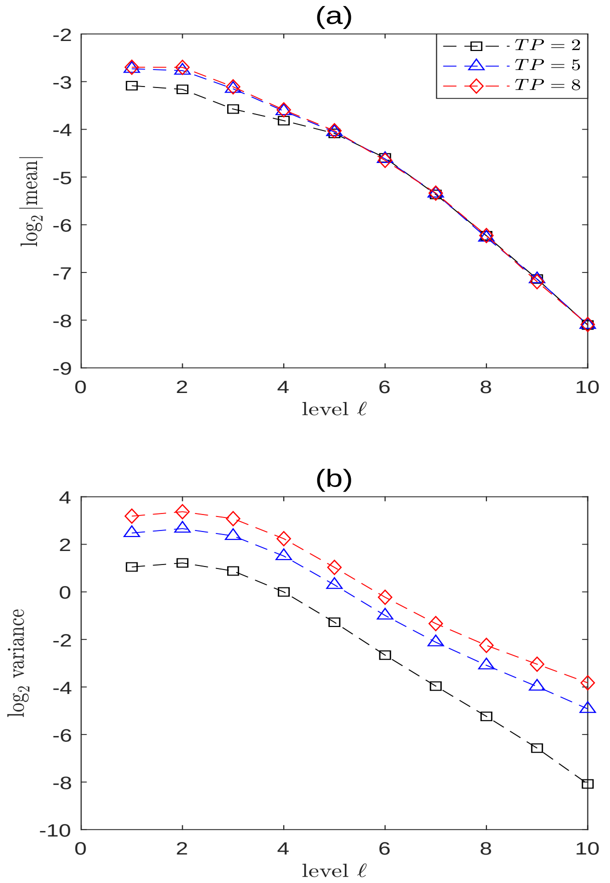

Fig. 7. Contrast Mean and Variance at Difference T Value

uses smaller levels to meet the required accuracy, which can be accepted despite the high kurtosis phenomenon.

Fig 6(b) shows the total computation cost of each method. For Theorem 1, if the complexity is located in $O(\epsilon^{-2})$, then the accuracy ϵ cannot influence $\epsilon^2 \times$ Cost. The plot of Fourier transform method is clearly a straight line, indicating that its complexity is $O(\epsilon^{-2})$ as anticipated. Additionally, the QMC method indeed helps to reduce the overall cost.

C. Different T Test

In the following section, we aim to investigate how different truncation points T affect the performance of Fourier transform MLMC method.

According to (24), Jin and Zhang [17] used an algorithm for determining the truncation point in integral

$$F_T(x) = \int_0^T \frac{1}{1+\pi^2 t^2}\{\mathbb{E}[e^{2V_x}\cos(2\pi t\tilde{V})] \\ \times (\cos(2\pi t) - \pi t \sin(2\pi t)) \\ - \mathbb{E}[e^{2V_x}\sin(2\pi t\tilde{V})] \\ \times (\sin(2\pi t) + \pi t \sin(2\pi t))\}\mathrm{d}t.$$

We used truncation points with different values to test the influence of T on selection. For this test, we selected three scenarios: $T = 2$, $T = 5$ and $T = 8$. We then plotted corresponding graphics to analyze them.

Fig 7 shows the empirical means and variances of estimation at various T values. The left plot shows that, despite some initial differences in the T value of the mean, at higher levels, they are almost indistinguishable. This indicates that the T value has a minimal impact on expectation. In the right plot, the variances for the three T values show a similar downward trend. When using the Monte Carlo method, smaller variance values result in better performance for the simulator estimator. Additionally, we believe that the $T = 2$ estimator has the highest performance.

Fig 8 displays the N_ℓ situation of three T values at five accuracy demands. With the increasing of T value, level sampling shows a consistent trend. For instance, when the error bound is $\epsilon = 0.005$, the N_{10} sampling is approximately 10^3 for the $T = 2$ case, nearly 10^4 for the $T = 5$ situation, and approximately 10^5 for the $T = 8$ scenario. Intuitively, we might expect the level to increase as the T value increases while maintaining identical accuracy. However, it is obvious that the $T = 5$ level is the smallest among the three T value scenarios. This is because the level value only influences the "fine" estimator $\tilde{P}_\ell$ but does not affect the computation cost and convergence rate significantly.

In Fig 9, we have plotted the test results of kurtosis

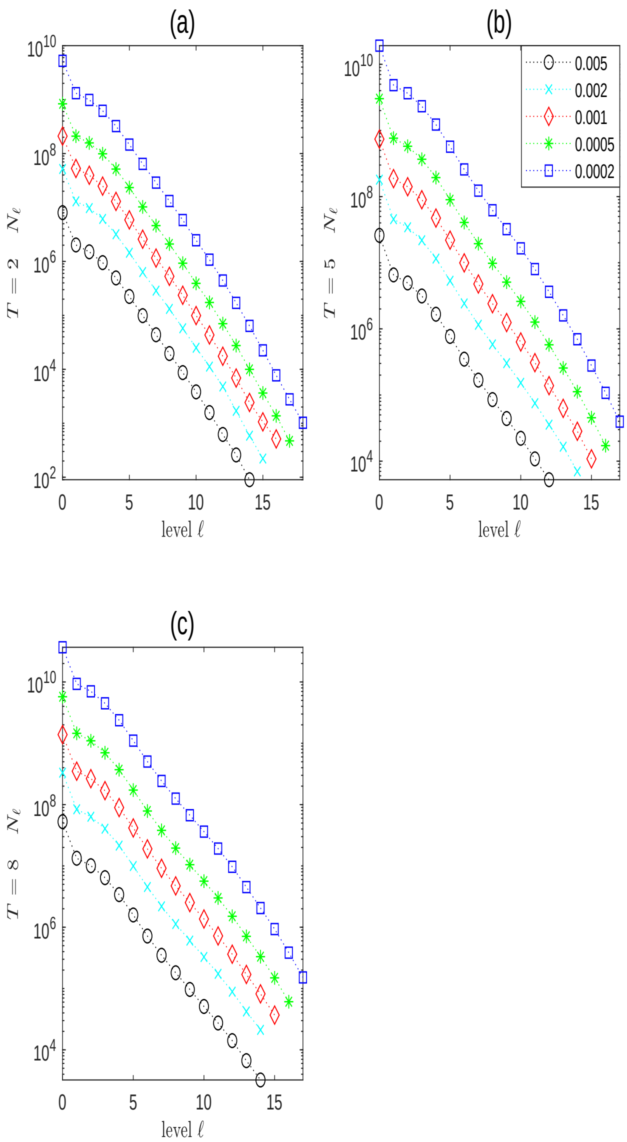

Fig. 8. Test of N_ℓ at three T values

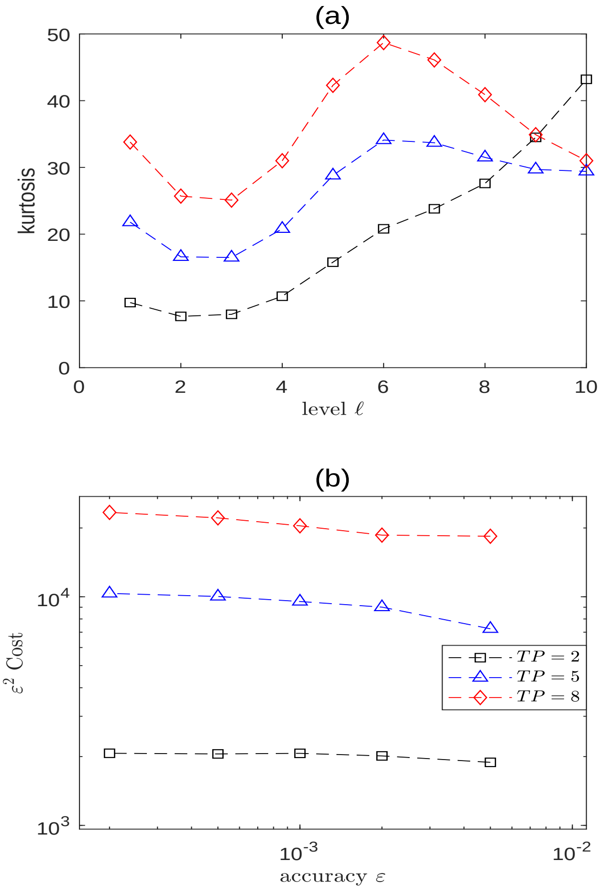

Fig. 9. Test of Kurtosis and Computation Cost

TABLE I
THE ESTIMATION RESULTS OF DIFFERENT T VALUES

accuracy	T = 2	T = 5	T=8
$\epsilon = 5 \times 10^{-3}$	0.1057	0.0944	0.1037
$\epsilon = 2 \times 10^{-3}$	0.0976	0.0963	0.1013
$\epsilon = 1 \times 10^{-3}$	0.0993	0.1007	0.0995
$\epsilon = 5 \times 10^{-4}$	0.0995	0.0998	0.1002
$\epsilon = 2 \times 10^{-4}$	0.1000	0.0999	0.1001

and computational cost. In the $T = 5$ and $T = 8$ cases, the kurtosis curve increases from the vertex and then decreases. In contrast, for the $T = 2$ scenario, the kurtosis curve continuously rises, but the maximum kurtosis for the $T = 2$ case is the lowest.

In the computational cost part, we observed that the three curves are almost straight lines. When the accuracy demand is $\epsilon = 2 \times 10^{-4}$, the $\epsilon^2 \times$ Cost is approximately $10^{3.2}$ for the $T = 2$ case, close to 10^4 for the $T = 5$ case, and around $10^{4.5}$ for the $T = 8$ case. In essence, as the T value increases, so does the computational cost. Fortunately, as we had hoped, the three computational complexities are $O(\epsilon^{-2})$. The phenomenon clearly shows the effectiveness of the Fourier transform method to some extent.

Table I illustrates the results of different T values used at various levels of accuracy. At coarse accuracy, the results are relatively larger and may exceed the accuracy limit. However, at the finest accuracy, we can observe that the estimators with the three T values are very close to or equal the true value of 0.1.

In summary, increasing T value does not necessarily improve the performance of the FMLMC method in all aspects. When considering the computation cost, it is recommended to select $T = 2$ as an optimal choice.

V. Conclusion

In this paper, we use the Fourier transform method to address financial risk estimation (1) via nested simulation. By substituting the indicator function with a smooth function, we employ the MLMC method to calculate the smooth function and derive the loss probability. In the numerical study, we observe that the complexity of the FMLMC method is $O(\epsilon^{-2})$. Additionally, by incorporating the QMC method into the FMLMC method, we achieve a better computation cost compared to the FMLMC method, which inevitably leads to the high kurtosis phenomenon. Finally, we investigate the influence of truncation point selection on the Fourier transform method.

It is expected that the FMLMC methods can be further improved in the following aspects. On one hand, we only applied RQMC method in the inner simulation. By utilizing the RQMC method in both inner and outer sampling, the computational cost may be significantly reduced. On the other hand, we used a fixed truncation point in the Fourier transform method. If we are able to find a suitable distribution function to apply the importance sampling method, it may reduce the estimation error and improve the accuracy of the results.

References

[1] X. Deng, Y. Lin, and H. Zhuang, "Uncertain portfolio with fuzzy investment proportion based on possibilistic theory," *Engineering Letters*, vol. 29, no. 2, pp. 803 – 812, 2021.

[2] M. B. Gordy and S. Juneja, "Nested simulation in portfolio risk measurement," *Management Science*, vol. 56, no. 10, pp. 1833–1848, 2010.

[3] M. Broadie, Y. Du, and C. C. Moallemi, "Efficient risk estimation via nested sequential simulation," *Management Science*, vol. 57, no. 6, pp. 1172–1194, 2011.

[4] Y. Li and G. Wen, "Research and practice of financial credit risk management based on federated learning," *Engineering Letters*, vol. 31, no. 1, pp. 271 – 278, 2023.

[5] L. Min, Y. Han, and Y. Xiang, "A two-stage robust omega portfolio optimization with cardinality constraints," *IAENG International Journal of Applied Mathematics*, vol. 53, no. 1, pp. 86–93, 2023.

[6] Broadie, Mark and Du, Yiping and Moallemi, Ciamac C, "Risk estimation via regression," *Operations Research*, vol. 63, no. 5, pp. 1077–1097, 2015.

[7] L. J. Hong, S. Juneja, and G. Liu, "Kernel smoothing for nested estimation with application to portfolio risk measurement," *Operations Research*, vol. 65, no. 3, pp. 657–673, 2017.

[8] M. B. Giles, "Multilevel monte carlo path simulation," *Operations Research*, vol. 56, no. 3, pp. 607–617, 2008.

[9] M. B. Giles and L. Szpruch, "Antithetic multilevel Monte Carlo estimation for multi-dimensional SDEs without Lévy area simulation," *The Annals of Applied Probability*, vol. 24, no. 4, pp. 1585 – 1620, 2014.

[10] M. B. Giles and A.-L. Haji-Ali, "Multilevel nested simulation for efficient risk estimation," *SIAM/ASA Journal on Uncertainty Quantification*, vol. 7, no. 2, pp. 497–525, 2019.

[11] M. B. Giles, "Mlmc for nested expectations," *Contemporary Computational Mathematics-A Celebration of the 80th Birthday of Ian Sloan*, pp. 425–442, 2018.

[12] M. B. Giles and T. Goda, "Decision-making under uncertainty: using mlmc for efficient estimation of evppi," *Statistics and Computing*, vol. 29, pp. 739–751, 2019.

[13] T. Goda, D. Murakami, K. Tanaka, and K. Sato, "Decision-theoretic sensitivity analysis for reservoir development under uncertainty using multilevel quasi-monte carlo methods," *Computational Geosciences*, vol. 22, pp. 1009–1020, 2018.

[14] T. Goda, T. Hironaka, and T. Iwamoto, "Multilevel monte carlo estimation of expected information gains," *Stochastic Analysis and Applications*, vol. 38, no. 4, pp. 581–600, 2020.

[15] G. Bakshi and D. Madan, "Spanning and derivative-security valuation," *Journal of Financial Economics*, vol. 55, no. 2, pp. 205–238, 2000.

[16] D. S. Bates, "Jumps and Stochastic Volatility: Exchange Rate Processes Implicit in Deutsche Mark Options," *The Review of Financial Studies*, vol. 9, no. 1, pp. 69–107, 2015.

[17] X. Jin and A. X. Zhang, "Reclaiming quasi–monte carlo efficiency in portfolio value-at-risk simulation through fourier transform," *Management Science*, vol. 52, no. 6, pp. 925–938, 2006.

[18] H. Niederreiter, *Random number generation and quasi-Monte Carlo methods.* SIAM, 1992.

[19] J. Dick, F. Y. Kuo, and I. H. Sloan, "High-dimensional integration: the quasi-monte carlo way," *Acta Numerica*, vol. 22, pp. 133–288, 2013.

[20] P. L'Ecuyer and C. Lemieux, "Recent advances in randomized quasi-monte carlo methods," *Modeling Uncertainty: An Examination of Stochastic Theory, Methods, and Applications*, pp. 419–474, 2002.

[21] M. B. Giles and B. J. Waterhouse, "Multilevel quasi-monte carlo path simulation," *Advanced Financial Modelling, Radon Series on Computational and Applied Mathematics*, vol. 8, pp. 165–181, 2009.

[22] F. Y. Kuo, C. Schwab, and I. H. Sloan, "Multi-level quasi-monte carlo finite element methods for a class of elliptic pdes with random coefficients," *Foundations of Computational Mathematics*, vol. 15, pp. 411–449, 2015.

[23] F. Kuo, R. Scheichl, C. Schwab, I. Sloan, and E. Ullmann, "Multilevel quasi-monte carlo methods for lognormal diffusion problems," *Mathematics of Computation*, vol. 86, no. 308, pp. 2827–2860, 2017.

[24] J. Dick, F. Y. Kuo, Q. T. Le Gia, and C. Schwab, "Multilevel higher order qmc petrov–galerkin discretization for affine parametric operator equations," *SIAM Journal on Numerical Analysis*, vol. 54, no. 4, pp. 2541–2568, 2016.

[25] R. Scheichl, A. M. Stuart, and A. L. Teckentrup, "Quasi-monte carlo and multilevel monte carlo methods for computing posterior expectations in elliptic inverse problems," *SIAM/ASA Journal on Uncertainty Quantification*, vol. 5, no. 1, pp. 493–518, 2017.

[26] I. H. Sloan, I. Sloan, and S. Joe, *Lattice methods for multiple integration.* Oxford University Press, 1994.

[27] A. B. Owen, "Randomly permuted (t, m, s)-nets and (t, s)-sequences," in *Monte Carlo and Quasi-Monte Carlo Methods in Scientific Computing: Proceedings of a conference at the University of Nevada, Las Vegas, Nevada, USA, June 23–25, 1994.* Springer, 1995, pp. 299–317.

[28] J. C. Hull, *Options, futures, and other derivatives.* Pearson, 2017.